Airfoil Flow Control Using DBD Plasma Actuators

X. N. Wang, W. B. Wang, Y. Huang, Z. B. Huang and Z. H. Sheng

Abstract Experiments were carried out to study the effect of plasma flow control on airfoil in an open-circuit low-speed wind tunnel. Lift and drag were measured by a five-component strain gauge balance. Particle image velocimetry (PIV) technology was applied to visualize the flow field over the airfoil. Influence of plasma actuator voltage, electrode position, and control evolution on NACA0015 airfoil was investigated, and the control mechanism was preliminarily analyzed. Lift enhancement validation experiment on NACA23018 two-element airfoil was carried out. The results show that the plasma actuators can efficiently increase the maximum lift and stall angle on a symmetric airfoil and a high-lift airfoil.

Keywords Flow control · DBD · Plasma

1 Introduction

Plasma technique has received much attention in recent decades due to its prospective applications in flow control (Roth et al. 1998). It can effectively control boundary-layer transition and separation, significantly improve lift-to-drag ratio and stall angle of the aircraft, etc (He et al. 2009). This work aims to investigate the influence of the control parameters, analyze the control mechanism, and validate the control effect on a high-lift airfoil.

X. N. Wang (✉) · W. B. Wang · Y. Huang · Z. B. Huang · Z. H. Sheng
China Aerodynamics Research and Development Center, Mianyang, Sichuan, China
e-mail: xunnian@sohu.com

X. N. Wang · W. B. Wang · Y. Huang · Z. B. Huang · Z. H. Sheng
State Key Laboratory of Aerodynamics, Mianyang, Sichuan, China

Y. Zhou et al. (eds.), *Fluid-Structure-Sound Interactions and Control*,
Lecture Notes in Mechanical Engineering, DOI: 10.1007/978-3-642-40371-2_20,

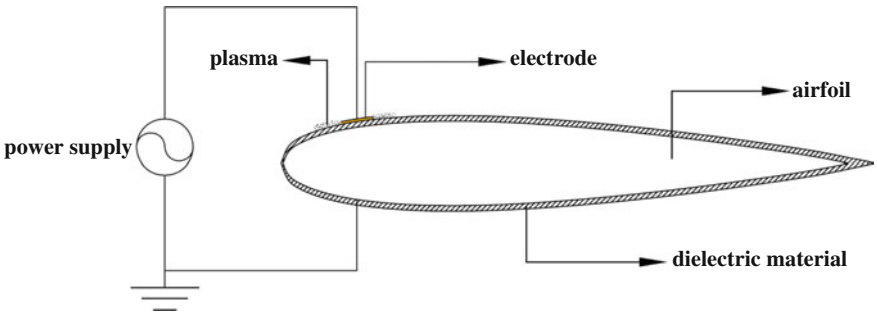

Fig. 1 The layout of the plasma actuator on NACA0015 airfoil

2 Experimental Details

The experiment was conducted in the drawdown open-circuit low-speed wind tunnel, with a test section of 0.7 m (width) × 0.7 m (height) × 1.05 m (length). The flow speed in the experiments ranges from 20 to 40 m/s. NACA0015 airfoil and NACA23018 two-element airfoil used in the experiment are both with a chord length of 0.1 m and a span of 0.48 m. The airfoils are both made of aluminum. Lift and drag were measured by a five-component strain gauge balance. Flow field was measured by particle image velocimetry (PIV).

Influence of plasma actuator voltage, electrode position, and control evolution is investigated on NACA0015 airfoil. Lift enhancement validation experiment is carried out on NACA23018 two-element airfoil.

The plasma actuator consists of two electrodes separated by three layers of 0.1-mm-thick Kapton film, as shown in Fig. 1. One of the electrodes is made of 0.05-mm-thick copper foil tape, and the other one is the whole airfoil model. The upper electrode is arranged along spanwise with a width of 2 mm and a length of 440 mm. The DBD plasma is operated in steady mode.

3 Results and Discussion

Figure 2 presents C_L and $C_D - C_L$ of NACA0015 airfoil at $V_\infty = 20$ m/s. The plasma actuator is located at $x/c = 0$ %. There is no visible lift enhancement on the airfoil at low angles of attack, but there is a significant lift increment at natural post-stall conditions. With control, $C_{L\max}$ and α_{stall} increase by 11 % and 6°, respectively, and lift-to-drag ratio improves as much as 199 %.

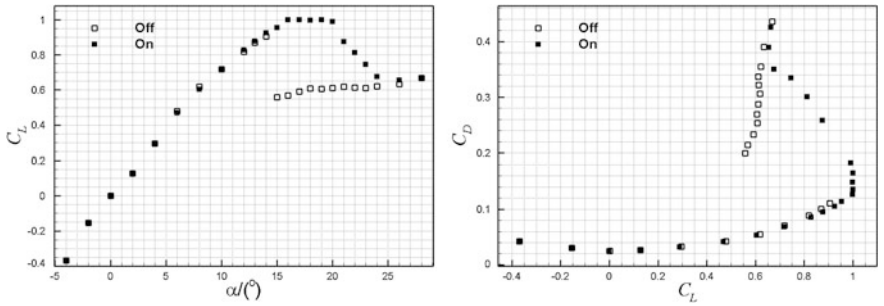

Fig. 2 Lift coefficient versus angle of attack (*left*) and drag polar (*right*) for the NACA0015 airfoil ($x/c = 0$ %, $V = 4.0$ kV, $f = 3.0$ kHz)

3.1 Power Parameters

Effect of the actuator voltages on C_L and C_D is shown in Fig. 3. When the actuator voltage is not high enough, there is no improvement on C_L and C_D. However, once a threshold voltage is reached, C_L increases and C_D decreases dramatically. Above this voltage, there is very little change in C_L and C_D.

The threshold value is 1.6 kV at $\alpha = 15°$ and 17°, while the value is 2.4 kV at $\alpha = 18°$. At higher attack angle, the flow separation is much stronger and flow control is more difficult, resulting in higher actuator voltage threshold value.

3.2 Electrode Position

Table 1 lists the locations about the plasma actuators. Figure 4 shows $C_{L\max}$ and α_{stall} increments for various actuator locations at different velocities. The actuator near the leading edge of the airfoil can significantly improve stall character. At the range of the control $(0 \leq x/c \leq 6\,\%)$, the actuator near the trailing edge, $C_{L\max}$, apparently increases more.

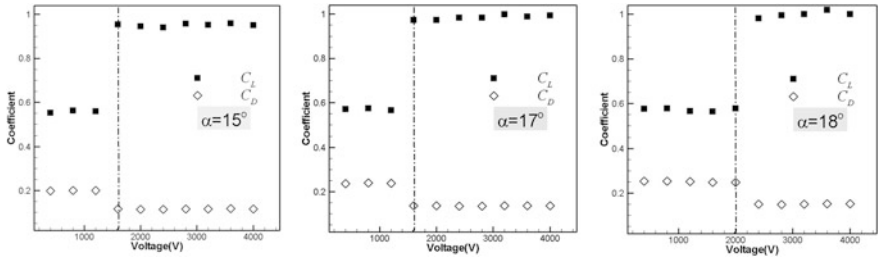

Fig. 3 Effect of the actuator voltages on the lift and drag coefficient ($x/c = 0$ %, $V_\infty = 20$ m/s, $f = 3.0$ kHz)

Table 1 The locations about the plasma actuators

Case	x/c (%)
1	0
2	1
3	3.5
4	6

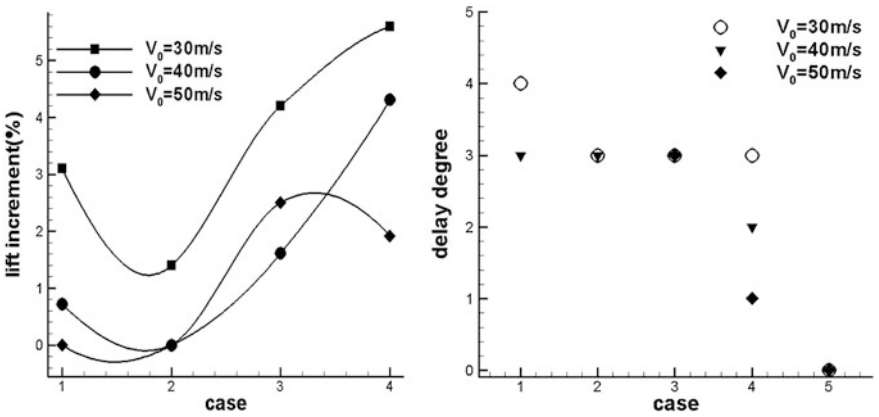

Fig. 4 $C_{L\max}$ and α_{stall} increments for various actuator locations at different velocities ($V = 4.0$ kV, $f = 3.0$ kHz)

3.3 Velocity Field

Figure 5 shows the time-averaged PIV results of the NACA0015 airfoil at $\alpha = 16°$ before and after control. A large separation region covers the upper surface without control, while the flow is observed to be attached all over the upper surface with control.

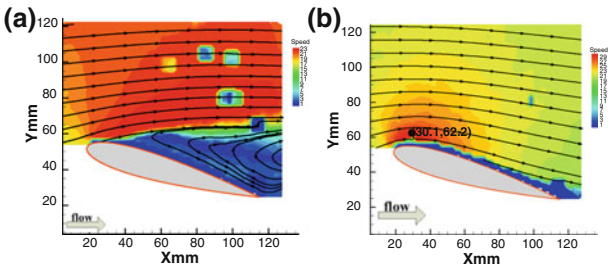

Fig. 5 PIV results of the NACA0015 airfoil: **a** plasma off; **b** plasma on ($\alpha = 16°, V_\infty = 20$ m/s, $x/c = 0\%$, $V = 2.4$ kV, $f = 3.0$ kHz)

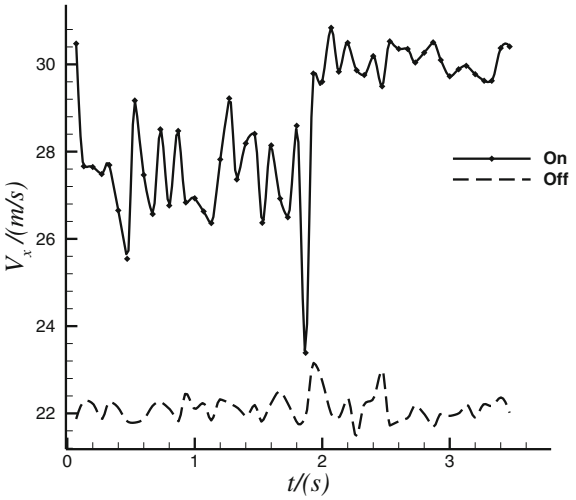

Fig. 6 The streamwise velocity evolution ($\alpha = 16°, V_\infty = 20$ m/s, $x/c = 0$ %, $V = 2.4$ kV, $f = 3.0$ kHz)

Figure 6 gives the streamwise velocity evolution at point (30.1, 62.2) (shown in Fig. 4b). The streamwise velocity is around an average of 22 m/s before control, while it increases significantly after control, which fluctuates around 27 m/s, and it is about 30 m/s after 2 s. The rule that the streamwise velocity changes with time agrees with that of the change of flow field. When the actuator is on, the plasma disturbs the flow, so the control is effective instantaneously. With the flow field unsteady variation and the ion transferring, the actuator voltage is not high enough to maintain the plasma to a steady state, so the flow control is unsteady during a certain time. After a period of time, the ion cumulates to a density achieving a balance, so the control is steady.

Figure 7 gives the streamwise velocity at different locations before and after control. When there is no separation at $\alpha = 14°$, the streamwise velocity at the upper surface is no meaningful different with and without control. When there is large separation without control and the flow is reattached with control at $\alpha = 16°$,

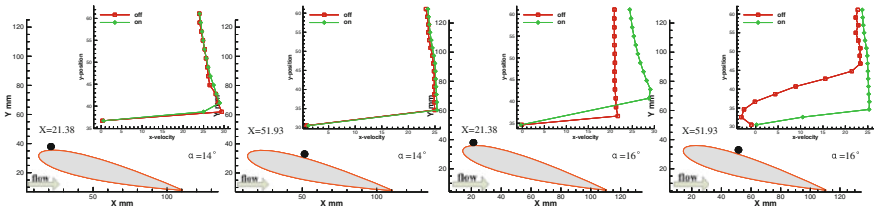

Fig. 7 The x-velocity at different locations before and after control ($V_\infty = 20$ m/s, $x/c = 0$ %, $V = 2.4$ kV, $f = 3.0$ kHz)

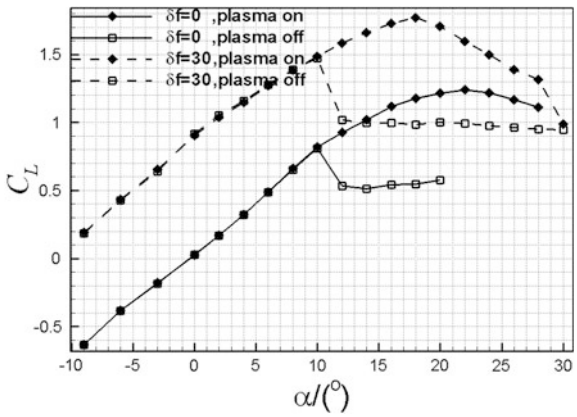

Fig. 8 Lift coefficient versus angle of attack for the NACA23018 two-element airfoil ($V_\infty = 20$ m/s, $V = 2.4$ kV, $f = 3.0$ kHz)

the streamwise velocity at the upper surface is obviously increased after control. The mechanism of the plasma flow control is believed to be producing a disturbance in the flow that makes the high velocity flow and low velocity flow become mixed, and the flow over the boundary layer injects into the boundary layer, so the boundary-layer transition is delayed and the flow separation is restrained.

3.4 Lift Enhancement Validation

Lift enhancement validation results of NACA23018 two-element airfoil are shown in Fig. 8. The plasma actuator is located at $x/c = 0.5$ %. When $V_\infty = 20$ m/s, $C_{L\max}$ increases 52 % and α_{stall} increases 12° with $\delta f = 0°$, and $C_{L\max}$ increases 18 % and α_{stall} increases 8° with $\delta f = 30°$. The plasma actuator has the same function as a leading-edge slat, and it can be used with other trailing-edge high-lift system, so it has a potential application foreground in the design of transport aircraft.

4 Conclusions

The leading-edge plasma actuators can efficiently increase $C_{L\max}$ and α_{stall} on a symmetric airfoil and a high-lift airfoil. At a given flow state, there exists threshold values for the actuator voltage on the actuator. The actuator located at different position has different contributions on $C_{L\max}$ and α_{stall}. The mechanism of the plasma flow control is believed to be producing a disturbance in the flow.

References

He C, Corke TC, Patel MP (2009) Plasma flaps and slats: an application of weakly ionized plasma actuators. J Aircr 46:864–873

Roth JR, Sherman DM, Wilkinson SP (1998) Boundary layer flow control with a one atmosphere uniform glow discharge surface plasma. AIAA, pp 1998–0328